

## Optical Reflectance of Polymeric Sulfur Nitride Films from the Ultraviolet to the Infrared\*

A. A. Bright, Marshall J. Cohen,† A. F. Garito, and A. J. Heeger

*Department of Physics and Laboratory for Research on the Structure of Matter, University of Pennsylvania, Philadelphia, Pennsylvania 19174*

and

C. M. Mikulski, P. J. Russo, and A. G. MacDiarmid

*Department of Chemistry and Laboratory for Research on the Structure of Matter, University of Pennsylvania, Philadelphia, Pennsylvania 19174*

(Received 23 September 1974)

We report the first synthesis of chemically pure polymeric sulfur nitride [(SN)<sub>x</sub>]. The optical reflectance of well-characterized films of this polymeric solid has been measured from the near ultraviolet (30 000 cm<sup>-1</sup>) to the far infrared (500 cm<sup>-1</sup>). Metallike reflectance is observed in the infrared through the visible region with a well-defined plasma minimum near 22 000 cm<sup>-1</sup>, corresponding to light polarized parallel to the polymer chain axis. The Drude-Lorentz model is used to analyze the data, and the physical implications of the resultant parameters are discussed.

Recently the dc electrical conductivity results of Labes and co-workers<sup>1</sup> (WLP) have raised the possibility that the polymeric solid (SN)<sub>x</sub><sup>2,3</sup> is another example of a one-dimensional conductor. Direct evidence from electron diffraction studies for the linear chain polymeric structure has been reported,<sup>4</sup> and recently Donohue<sup>5</sup> has confirmed the structure in initial x-ray diffraction studies.

We have found that (SN)<sub>x</sub> can be formed as highly reflective thin films having a golden lustrous appearance and the same structure as crystalline (SN)<sub>x</sub>. We report here the frequency dependence of the reflectance of (SN)<sub>x</sub> films from 30 000 to 500 cm<sup>-1</sup>. The results are used to draw important conclusions regarding the electronic structure of this unique material.

Following a modification of the method of WLP,<sup>1</sup> lustrous brass-colored crystalline (SN)<sub>x</sub> was prepared by slow polymerization of S<sub>2</sub>N<sub>2</sub> crystals at 0°C under 1 atm of argon over a three day period. The resulting (SN)<sub>x</sub> crystals were then subjected to constant pumping (<10<sup>-3</sup> Torr) for several hours to remove any traces of unchanged S<sub>2</sub>N<sub>2</sub>. Suitable crystals appeared golden in color; any copper-colored crystals were discarded as impure. A more detailed description of the synthesis will be presented elsewhere.<sup>6</sup>

Analysis of crystals of (SN)<sub>x</sub> was as follows.<sup>7</sup> Calculated: S, 69.59; N, 30.41. Found: S, 69.29, 70.18; N, 30.56, 30.20. The duplicate analyses were for crystals obtained from different experiments. Specific analyses were carried out for C, H, and O, all of which were found to be absent. Emission spectrographic analyses showed

no measurable metal impurities (<5 ppm).

Although the (SN)<sub>x</sub> crystals appeared shiny, careful examination showed that the surfaces were strongly striated, appearing fibrous under a microscope (100–500×). The electron micrographs of (SN)<sub>x</sub> crystals in Fig. 1 clearly show the fibrous nature of the material. What appears to be a macroscopic single crystal, in fact, consists of oriented bundles of fibers. As a result, incident light was scattered widely, making quantitative measurements on such crystals impracticable.

It was possible, however, to make several qualitative observations. Under polarized light, the reflectance was found to be highly anisotropic. A gold metallic luster was observed with polarization parallel to the fibers, whereas under

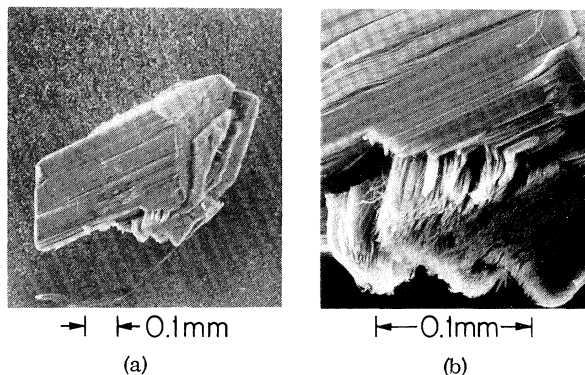


FIG. 1. Electron micrographs of (SN)<sub>x</sub>. (a) An imperfect single crystal. (b) Higher magnifications showing striations described in the text.

transverse polarized light the crystals appeared dark blue-black.

Thin films of  $(\text{SN})_x$  (a few microns thick) were formed by sublimation of crystalline  $(\text{SN})_x$  in a vacuum sublimator ( $<10^{-4}$  Torr and  $130\text{--}150^\circ\text{C}$ ). Glass substrates were held at  $27^\circ\text{C}$  by mounting them on a water-cooled cold finger in the sublimator.

Debye-Scherrer patterns of the film and of crystalline  $(\text{SN})_x$  were identical and agreed with published x-ray data for polycrystalline  $(\text{SN})_x$ .<sup>8</sup> No lines characteristic of either  $\text{S}_4\text{N}_4$ <sup>9</sup> or  $\text{S}_2\text{N}_2$ <sup>8</sup> were present in either type of  $(\text{SN})_x$  samples. It should be noted that occasionally some  $\text{S}_4\text{N}_4$  was formed in the earliest films prepared, and was subsequently avoided in later films by empirically refining the film growth conditions. The presence of  $\text{S}_4\text{N}_4$  had no effect on the visual appearance of the films, so that each film was examined individually by x-ray techniques.

From diffractometer measurements of  $(\text{SN})_x$  films on glass, the striking result was found that the films grow preferentially oriented with the  $(\bar{1}02)$  plane parallel to the substrate surface. The mean plane of the  $(\text{SN})_x$  polymer chains is also  $(102)$ ,<sup>4</sup> indicating that the conducting axis lies in the plane of the film. When examined under a microscope, the films had the same gold appearance as crystalline  $(\text{SN})_x$ , but exhibited a high-quality reflective surface. The films consist of randomly oriented crystallites with a grain size of order  $1\ \mu\text{m}$ . Under polarized light, each grain of the film appeared reflective at some angle of the polarizer, confirming that the chain direction of each grain lay in the plane of the film. Scanning electron micrographs are consistent with these conclusions, and show that the films are smooth on the scale of thousands of angstroms. On the basis of observing oriented growth on glass, we anticipate that further studies will likely demonstrate that epitaxial films of this polymeric solid can be grown on suitable oriented substrates.

Reflectance measurements were carried out as described earlier.<sup>10</sup> In all cases, care was taken to avoid prolonged exposure of the samples to air.

The extreme optical anisotropy observed for crystalline  $(\text{SN})_x$  is similar to that found in electronically one-dimensional materials.<sup>10-14</sup> Metallic behavior is observed for polarization parallel to the principal conducting axis and insulating properties in the perpendicular direction. Accordingly, the assumption is made that the ob-

served  $(\text{SN})_x$  reflectance can likewise be approximated as an average of longitudinal (metallic) and transverse (insulating) components:

$$R_{\text{measured}} = (R_{\parallel} + R_{\perp})/2 \quad (1)$$

with the transverse component independent of frequency.

For metallic behavior, the Drude dielectric function  $\epsilon(\omega)$  is given by

$$\epsilon(\omega) = \epsilon_{\text{core}} - \omega_p^2 / (\omega^2 + i\omega/\tau) \equiv \epsilon_1 + i\epsilon_2, \quad (2)$$

where

$$\omega_p^2 = 4\pi N e^2 / m^*. \quad (3)$$

$\epsilon_{\text{core}}$  is the residual dielectric constant at high frequency arising from core polarizability,  $\tau$  is the electronic relaxation time,  $\omega_p$  is the plasma frequency,  $N$  is the electron density, and  $m^*$  is the optical effective mass. In terms of the real and imaginary parts of  $\epsilon$ , the reflectance is given by

$$R = \frac{1 + |\epsilon| - [2(|\epsilon| + \epsilon_1)]^{1/2}}{1 + |\epsilon| + [2(|\epsilon| + \epsilon_1)]^{1/2}}, \quad (4)$$

where  $|\epsilon| = (\epsilon_1^2 + \epsilon_2^2)^{1/2}$ .

The parameters  $\epsilon_{\text{core}}$ ,  $\omega_p$ , and  $\tau$  were determined by a least-squares fit of Eqs. (1), (2), and (4) to the experimental data near the plasma edge. The best fit was obtained with  $\epsilon_{\text{core}} = 1.46$ ,  $\omega_p = 4.3 \times 10^{15}\ \text{sec}^{-1}$  ( $\hbar\omega_p = 2.8\ \text{eV}$ ), and  $\tau = 1.9 \times 10^{-15}\ \text{sec}$ . The calculated reflectance based on these values is compared with the experimental results in Fig. 3. The extrapolation to high and low frequencies is shown in Fig. 2. The fit is

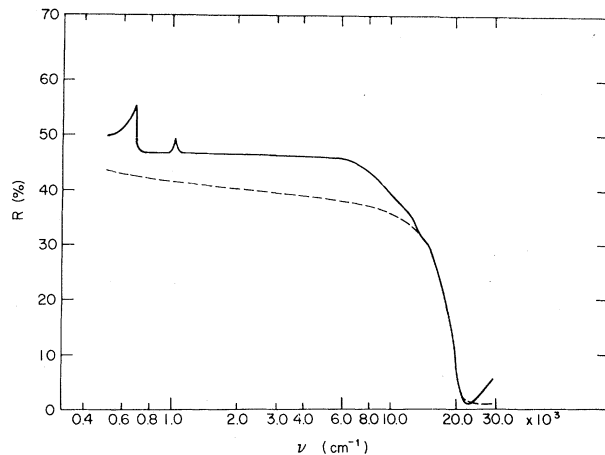


FIG. 2. Reflectance spectrum of a thin film of  $(\text{SN})_x$  from  $500\ \text{cm}^{-1}$  to  $30\,000\ \text{cm}^{-1}$ . Dashed line: Drude fit to the measured reflectance (see text). The structure at  $995$  and  $685\ \text{cm}^{-1}$  is related to S-N stretching modes.

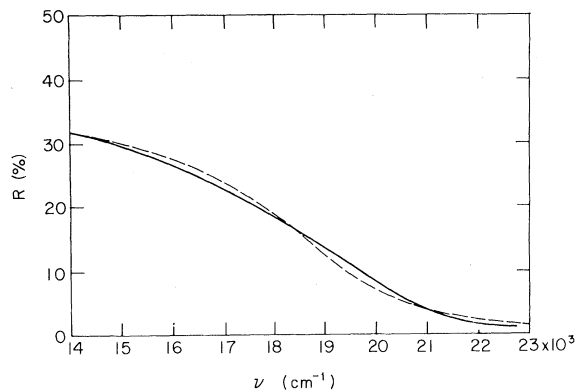


FIG. 3. Solid line: Reflectance of  $(\text{SN})_x$  thin film. Dashed line: Drude fit to the measured reflectance (see text).

very good in the vicinity of the plasma edge, but falls below the data at high frequencies ( $> 23\,000\text{ cm}^{-1}$ ). Attempts to improve the fit in this region led to an unreasonably high value for  $\epsilon_{\text{core}}$  ( $> 5$ ). The upturn in the reflectance at high frequencies may be due to an interband transition or to structure originating from the transverse direction. The fit also falls below the measured data in the infrared,  $\nu < 14\,000\text{ cm}^{-1}$ , suggesting that in this region as well there may be an increased transverse reflectance. Such an effect might be expected if interchain coupling were strong enough to give a metallic transverse conductivity and reflectance.

The fit with the Drude expression (2) is *not* unique. An equally good fit over the frequency range of Fig. 3 may be obtained by using a Drude-Lorentz dielectric function appropriate to a small-gap semiconductor. In this case, the dielectric function is given by

$$\epsilon(\omega) = \epsilon_{\text{core}} + \frac{\omega_p^2}{\omega_0^2 - \omega^2 - i\omega/\tau},$$

with values for  $\epsilon_{\text{core}}$ ,  $\omega_p$ , and  $\tau$  similar to the Drude values. However, the high reflectance throughout the infrared region limits acceptable values of  $\hbar\omega_0$  to less than 0.1 eV. Such a small energy gap would have a minor effect on the optical spectrum of Fig. 2.

In the case that the Drude expression [Eq. (2)] applies,<sup>15</sup> several important properties of  $(\text{SN})_x$  may be calculated. The dc conductivity of a metal is related to the plasma frequency and scattering time  $\tau$  by the relation,  $\sigma = \omega_p^2 \tau / 4\pi$ . Using the above values for  $\omega_p$  and  $\tau$ , one obtains an estimate of  $3 \times 10^3 (\Omega\text{ cm})^{-1}$  for the conductivity

along the polymer chains. This result is in fair agreement with reported room-temperature dc conductivity values of up to  $2 \times 10^3 (\Omega\text{ cm})^{-1}$ .<sup>1</sup> The effective mass  $m^*$  can be found from Eq. (3). With use of the value of  $N = 3 \times 10^{22}\text{ cm}^{-3}$  calculated from x-ray data,<sup>4,5</sup>  $m^*$  is found to be  $5.2m_e$ , where  $m_e$  is the free-electron mass. This result implies a relatively narrow band structure with a bandwidth on the scale of a few tenths of an eV.<sup>6</sup> However, static magnetic susceptibility measurements<sup>16</sup> carried out in our laboratory on crystalline and thin-film samples of  $(\text{SN})_x$  imply a density of states which is approximately an order of magnitude smaller than would be expected from a simple narrow energy band. Two possible explanations may account for this inconsistency: (1) The plasma edge observed in the visible may arise from an interband transition and not from free-carrier plasma oscillations, or (2) the susceptibility may be associated with a highly structured density of states.

\*Work supported in part by the National Science Foundation through the Laboratory for Research on the Structure of Matter, and Grants No. GH-39303 and No. GP-41766X, and by the Advanced Research Projects Agency through Grant No. DAHC 15-72C-0174.

†Submitted in partial fulfillment of the requirements for the Ph. D.

<sup>1</sup>V. V. Walatka, Jr., M. M. Labes, and J. H. Perlstein, Phys. Rev. Lett. **31**, 1139 (1973).

<sup>2</sup>F. B. Burt, J. Chem. Soc., London, Abstr. **1910**, 1171.

<sup>3</sup>For a review of sulfur nitrides, see H. G. Heal, Advan. Inorg. Chem. Radiochem. **15**, 375 (1972).

<sup>4</sup>M. Boudeulle and P. Michel, Acta Crystallogr., Sect. A **28**, S199 (1972); M. Boudeulle, A. Douillard, P. Michel, and G. Vallet, C. R. Acad. Sci., Ser. C **272**, 2137 (1971); M. Boudeulle and A. Douillard, J. Microsc. (Paris) **11**, 3 (1971).

<sup>5</sup>J. Donohue, to be published.

<sup>6</sup>C. M. Mikulski, P. J. Russo, A. G. MacDiarmid, A. F. Garito, and A. J. Heeger, to be published.

<sup>7</sup>The first set of analyses were performed by Gailbraith Laboratories, Inc., Knoxville, Tenn. 37921, and included specific analyses for carbon, hydrogen, and oxygen. The second set of analyses were performed by Schwarzkopf Microanalytical Laboratory, Woodside, N. Y. 11377, and were for sulfur and nitrogen only.

<sup>8</sup>M. Goehring and D. Voigt, Z. Anorg. Allg. Chem. **285**, 181 (1956).

<sup>9</sup>R. D. Sharma and J. Donohue, Acta Crystallogr. **16**, 891 (1963).

<sup>10</sup>A. A. Bright, A. F. Garito, and A. J. Heeger, Solid State Commun. **13**, 943 (1974), and Phys. Rev. B **10**, 1328 (1974).

<sup>11</sup>P. M. Grant, R. L. Greene, G. C. Wrighton, and G. Castro, *Phys. Rev. Lett.*, **31**, 1311 (1973).

<sup>12</sup>D. B. Tanner, C. S. Jacobsen, A. F. Garito, and A. J. Heeger, *Phys. Rev. Lett.*, **32**, 1301 (1974).

<sup>13</sup>D. Kuse and H. R. Zeller, *Phys. Rev. Lett.* **27**, 1060 (1971).

<sup>14</sup>H. P. Geserich, H. D. Hausen, K. Krogmann, and P. Stampfl, *Phys. Status Solidi (a)* **10**, 537 (1972).

<sup>15</sup>For a discussion of the applicability of the Drude expression to a narrow-band, one-dimensional system, see Ref. 10.

<sup>16</sup>J. C. Scott, private communication.

## Spin-Flip-Plus-Phonon Raman Scattering: A New Second-Order Scattering Process\*

R. L. Hollis, J. F. Ryan,† and J. F. Scott

*Department of Physics and Astrophysics, University of Colorado, Boulder, Colorado 80302*

(Received 29 October 1974)

A new second-order light scattering process has been observed which yields line spectra at frequency shifts  $\omega_{LO} \pm \omega_{SF}$ , where  $\omega_{LO}$  is a longitudinal optical-phonon frequency, and  $\omega_{SF}$  is an electron or hole spin-flip frequency. The scattering is highly resonant, and the proposed mechanism is analogous to that for multiple-phonon line spectra and double spin-flip scattering.

Second-order light scattering processes involving phonons<sup>1</sup> or magnons<sup>2</sup> usually produce continuum spectra with spectral intensity related to the two-particle joint density of states at each frequency  $\omega$ . Under resonant conditions, however, in which the incident or scattered photon energy matches that of the band gap or of other allowed dipole transitions in the scattering medium, second-order line spectra are observed. These line spectra are noteworthy in that they are exact replicas of the first-order  $q \approx 0$  scattering features. Such second- and higher-order processes have been studied in considerable detail in the case of phonon scattering in II-VI and III-V semiconductors<sup>3</sup> and were first analyzed from a theoretical standpoint by Loudon.<sup>4</sup> Other examples of second-order line spectra are those due to double spin-flip scattering. In *n*-CdS, light scattering from electrons in spin-split shallow-donor energy levels is observed in up to third order with laser excitation slightly below the direct band gap.<sup>5</sup>

In this Letter we present data on *p*-ZnTe obtained with above-band-gap excitation but with scattered photons having energy slightly lower than  $E_G$ . In addition to the hole spin-flip scattering observed recently in this material,<sup>6</sup> and the multiphonon line spectra previously reported,<sup>3</sup> we see a completely new process in which scattered photons are shifted to lower energy by  $\omega_{LO} \pm \omega_{SF}$ , where  $\omega_{LO}$  is the longitudinal optical-phonon frequency, and  $\omega_{SF}$  is the hole or electron spin-flip frequency. These spin-flip lines then appear as magnetic-field-dependent sidebands of

the LO phonon. Figure 1 shows the spectrum obtained at  $T=1.9$  K with applied magnetic field  $H=130$  kG. The experimental details are the same as in Ref. 6. The laser excitation energy is 2.410 eV and  $E_G=2.388$  eV<sup>7</sup>; the latter is indicated by the arrow at  $\sim 175$  cm<sup>-1</sup> below the laser line. The features at 183 and 211 cm<sup>-1</sup> are due to first-order scattering from TO and LO phonons, respectively, and agree well with earlier measurements. The sharp line at 422 cm<sup>-1</sup> is two-LO-phonon scattering and the weak feature at 394 cm<sup>-1</sup> corresponds to  $\omega_{LO} + \omega_{TO}$ . Free-exciton luminescence appears as a broad line centered at 288 cm<sup>-1</sup>. Not shown in the figure is a small magnetic field splitting of the free exciton, but this is apparent in its one-LO-phonon replica at 499 cm<sup>-1</sup>. In the low-frequency region near the laser line, weak spin-flip lines are observed, but their intensities are small as a result of very

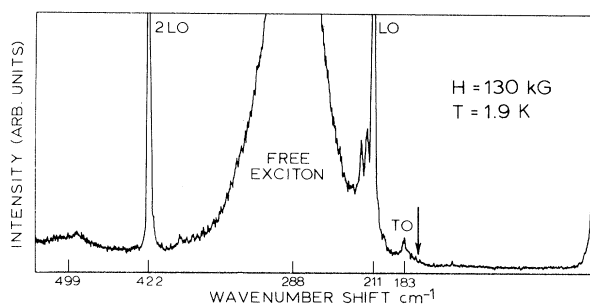


FIG. 1. Raman and luminescence spectrum of ZnTe obtained with  $\hbar\omega_L=2.410$  eV.  $E_G$  is indicated by the arrow. For a description of the various features see text.

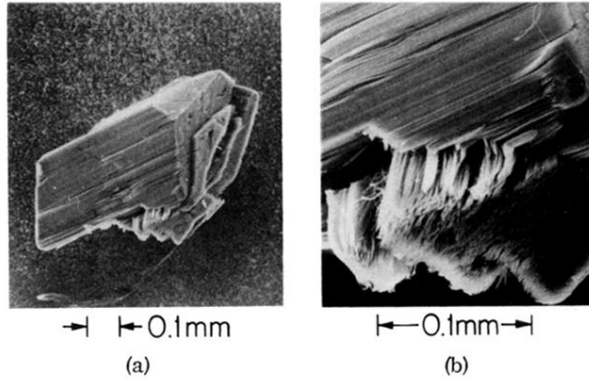


FIG. 1. Electron micrographs of  $(\text{SN})_x$ . (a) An imperfect single crystal. (b) Higher magnifications showing striations described in the text.